PERGAMON

Quaternary Science Reviews 21 (2002) 1099–1110

QG QSR

Multi-isotopic age assessment of dirty speleothem calcite: an example from Altamira Cave, Spain

Maylis Labonne[a,*], Claude Hillaire-Marcel[a], Bassam Ghaleb[a], Jose-Luis Goy[b]

[a] *GEOTOP, Université du Québec à Montréal, C.P.8888, Succursale Centre-Ville, Montréal, Québec, Canada, H3C 3P8*
[b] *Depto. de Geodinamica, Universidad de Salamanca, Spain*

Received 12 March 2001; accepted 2 September 2001

Abstract

The dating of dirty speleothem calcite of Late Pleistocene or Holocene age can be problematic. This is notably the case with the ^{14}C method, due to uncertainties in the initial ^{14}C activity of the cave CO_2, and with the ^{230}Th–^{234}U method, due to either low U contents in the authigenic calcite, and/or to the presence of heterogeneous detrital particles containing high concentrations of U and Th series isotopes frequently out of secular equilibrium. In this study of a $\sim$60 cm-thick flowstone sealing archaeological remains of the Magdalenian period in the Altamira Cave (NW Spain), we used a combination of isotopic approaches and analytical techniques to confront dating methods and finally tried to validate chronological interpretations based on stable isotope paleoclimate constraints. U-series data indicate the presence of a relatively important and heterogeneous detrital fraction resulting in $^{232}Th/^{230}Th$ mass ratios generally too high ($0.1–0.25 \times 10^6$) to allow precise TIMS measurements. MC-ICP-MS measurements provided more reliable results and allowed the calculation of ^{230}Th–^{234}U isochron ages of 11.8 ± 0.8 ka in the upper part of the flowstone, and of $\sim$22 ka, in the lower part of it. In view of the calibrated ^{14}C ages of these layers ($\sim$13 and $\sim$15 ka BP, respectively), the isochron age of the lower unit of the flowstone seems erroneous, suggesting the presence of an isotopically heterogeneous contaminating fraction in this layer. $^{226}Ra/^{230}Th$ ratio measurements indicate near secular equilibrium conditions. Seriate stable isotope measurements indicate calcite precipitation in isotopic equilibrium with ambient waters. They suggest that flowstone deposition ended at the very onset of the Younger Dryas. This transition seems to have occurred here at 11.8 ± 0.8 ($\pm 2\sigma$) ka (based on Th/U isochron), and 10.7 ± 0.08 ($\pm 1\sigma$) uncalibrated ^{14}C kiloyears. The ^{14}C activity for the cave CO_2 seems to have been near that of atmospheric CO_2 during the precipitation interval. It is concluded that the ^{14}C data provide here relatively reliable ages, in spite of the fact that they partly fall into a period characterized by ^{14}C-plateau effects, but that other isotopic data revealed essential in validating them.

1. Introduction

Several studies have demonstrated the interest of speleothems (stalagmites, flowstones) for the study of Late Quaternary palaeoenvironments (Gascoyne, 1992; Winograd et al., 1992; Goede, 1994; Bar-Matthews et al., 1996; Dorale et al., 1998; Hellstrom et al., 1998; Hellstrom and McCulloch, 2000). At the time scale of the last few tens of thousand years, ^{14}C measurements may provide relatively precise ages. However in karst systems, due to bedrock dissolution the contribution of "dead carbon" may result in $\Delta^{14}C$ values as high as 300‰ between atmospheric CO_2 and the cave equilibrating-CO_2 (Gewelt, 1986; Genty and Massault, 1997). Due to recent improvements in analytical methods (Li et al., 1989), U-series isotopes now offer a highly competitive approach, even for the dating of recent and/or U-poor speleothems (Ludwig et al., 1992; Hellstrom et al., 1998; Kaufman et al., 1998; Desmarcheliers et al., 2000; Vesica et al., 2000).

Several important criteria must be fulfilled for the direct determination of ^{230}Th–^{234}U ages in speleothem calcite: (1) no "detrital" ^{230}Th should be incorporated into calcite when it forms, (2) afterwards, the system must remain chemically closed to radionuclide migration (Li et al., 1989; Dorale et al., 1992; Ludwig et al., 1992; Stein et al., 1993; Kaufman et al., 1998). The presence of contaminating detrital particles is normally revealed by the relatively high abundance of ^{232}Th. However, correction for such detrital contributions can be achieved using the isochron approach (Kaufman and Broecker, 1965; Rosholt, 1976; Ku et al., 1979; Hillaire-Marcel and Causse, 1989; Schwarcz and Latham, 1989;

*Corresponding author. Tel.: +514-987-4080; fax: +514-987-3635.
E-mail address: c3551@er.uqam.ca (M. Labonne).

0277-3791/02/$ - see front matter
PII: S0277-3791(01)00076-2

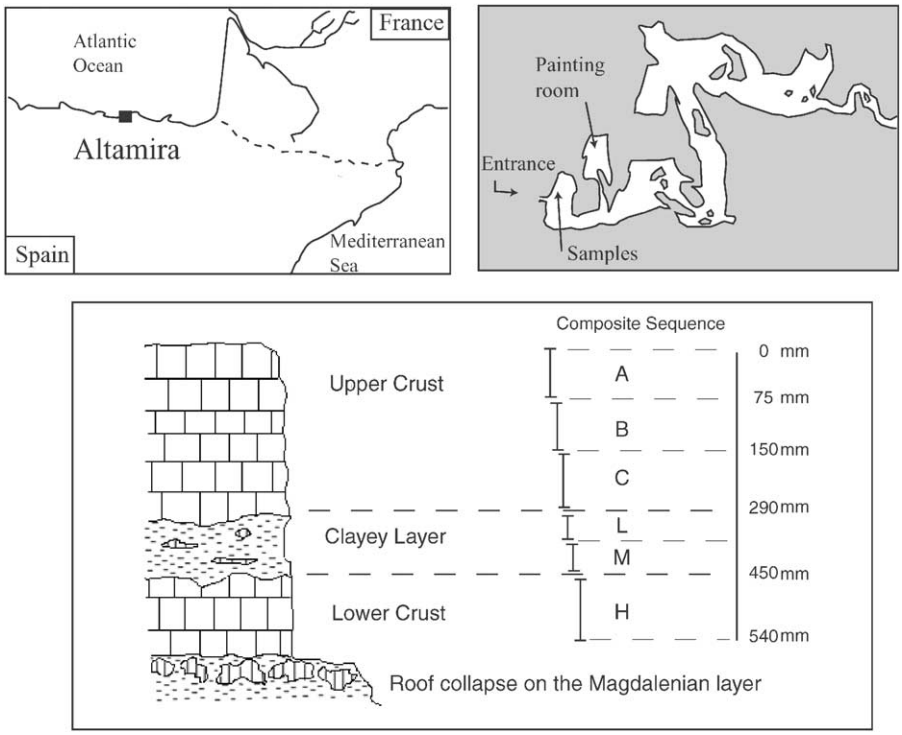

Fig. 1. Location of the Altamira Cave, and location of the flowstone sequence in the cave.

Bischoff and Fitzpatrick, 1991; Luo and Ku, 1991). These are usually based on the assumption that the initial isotopic composition of the detrital fraction in the sample is uniform and that the contaminating fraction is proportional to the ^{232}Th content of the sample. This is not always true, notably in cases where the contaminating particles are partly composed of reworked carbonate particles that are usually rich in U-series isotopes but poor in ^{232}Th (e.g., Hillaire-Marcel et al., 1995).

In this study, we examine the geochemical properties of a flowstone sealing archaeological remains in the Altamira Cave (northwestern Spain) with the objective of dating the depositional interval, in order to obtain a final minimum age for the human occupation of the cave. This cave, located in the Cantabrian mountains (Fig. 1), is well known for its rupestral art and related archaeological remains that have contributed to the evidence of human development during the Magdalenian Period (Straus, 1975; Moure-Romanillo and Cano-Herrera, 1979; Conkey, 1980). The cave ceiling collapsed at the end of the Magdalenian occupation, closing the entrance of the cave and burying all remains of earlier human occupation. The flowstone cements boulders fallen from the ceiling. Previous radiocarbon dating of archaeological remains, such as bones or charcoal, yielded (uncalibrated) ages ranging between ~15,960 and 14,480 B.P. (Almagro and Fernandez-Miranda, 1978). More recently, Valladas et al., 1992, reported (uncalibrated) ^{14}C ages of ca 14,000 B.P. for charcoal remains used for the cave paintings.

It seems unlikely that during the Magdalenian settlement, the ^{14}C activity of the cave CO_2 had been significantly lower than that of the atmospheric CO_2, because of the open ventilation required for human occupation. However, after the sealing of the cave entrance, i.e., during the deposition of the flowstone, the cave CO_2 activity may have decreased due to isotopic exchange with ^{14}C-depleted dissolved carbon from recharge waters and to radioactive decay. Therefore, we decided to compare ^{14}C-AMS and ^{226}Ra–^{230}Th–^{234}U ages in the flowstone, using data sets obtained from different analytical methods (TIMS: thermal ionization mass spectrometry, alpha spectrometry and MC-ICP-MS: multi collector inductively coupled mass spectrometer). We also made seriate stable isotope measurements for the reconstruction of paleoclimate conditions during the deposition of the flowstone, in order to compare radiometric ages with established regional paleoclimate records.

2. Material and methods

The flowstone covering the major Magdalenian archaeological remains was sampled in the vestibule to the left of the cave entrance (Fig. 1). The flowstone layer is about 50–70 cm thick and consists of three major units. The top and bottom ones present laminaes with a relatively well crystallized calcite. The intermediate unit is essentially clayey, but it contains abundant carbonate

nodules. During sampling, the top layer was split into three distinct layers, identified as A, B and C, from top to bottom. A, and B consist of a well laminated calcite, whereas C tends to be more porous at its top and shows evidence for the cementation of abundant detrital particles, at its base. The intermediate clayey rich layer yielded two samples (identified by the letters L and M; Fig. 1). The bottom unit H consists of a relatively homogeneous calcitic layer with lesser visible laminaes and large calcite crystals.

2.1. Stable isotope analyses

Subsampling for stable isotope measurements was made at ~5 mm-intervals throughout layers A, B, C and H. Approximately 0.5 mg of calcite powder was ground using a thin file. The analyses were performed using an Isocarb™ preparation device in line with a triple collector VG- PRISM™ mass spectrometer. Results are expressed as $\delta^{18}O$ and $\delta^{13}C$, in per mil with respect to the V-PDB standard (Coplen, 1995). The overall analytical reproducibility as determined on replicate measurements of laboratory standards is routinely better than $\pm 0.05\%$ ($\pm 1\sigma$), both for ^{18}O and ^{13}C.

2.2. U–Th analyses

Subsampling for ^{238}U, ^{234}U, ^{232}Th, ^{230}Th series measurements was made at 12 different depths (Fig. 3). All sub-samples were heated at 500°C for 4 h in order to carbonize any traces of organic matter, then crushed into fine powder. Relatively large samples were needed, especially for ^{230}Th measurements, due to the relatively young age of the carbonate and to its low U content. In addition, due to technical difficulties encountered during the course of the U and Th series analyses, three different analytical methods had to be used. We used first, whenever possible, TIMS. Some of these analyses were inconclusive, due to the difficulty of measuring the low ^{230}Th contents in the samples. In these cases, alpha spectrometry measurements provided more precise data about ^{230}Th activities. Unfortunately, the analytical uncertainty associated with alpha counting was generally too large to allow precise isochron age calculations. Finally, the acquisition of an MC-ICP-MS Isoprobe™ instrument, during the course of our study, allowed us to complete our data set using this instrument.

Approximately 30 g of material was used for each TIMS analysis, ~15 g for alpha-spectrometry and ~1 g for each MC-ICP-MS measurements. U and Th extraction on all samples, and notably on those used to calculate isochrons, was done after total sample dissolution (TSD). Indeed, different studies indicate that significant and unpredictable transfer of radionuclides may occur from the detritus to the leachate during most leaching procedures (Bischoff and Fitzpatrick, 1991; Luo and Ku, 1991). All samples were dissolved in a mixture of HCl and HNO_3 followed by HF. Most samples were completely dissolved. In a few cases, notably in layers L + M and to a lesser extend C, the presence of residual gel was noticed. In order to insure the most entire recovery of U and Th, the gel was washed with 6N HCl (2 or 3 times) and was loaded on the resin column after centrifugation of the solution. Therefore, we assumed that the recovery was complete. Analytical procedures for U and Th chemical extraction involved two stages. For the first one, the U and Th separation stage, we used a Biorad AG 1×8™ resin with 6N HCl and H_2O. In the second stage, for the purification of each metal, we used respectively a U/Teva™ resin with 0.02N HNO_3, for U, and a AG 1×8™ resin with 6N HCl, for Th (Carter et al., 1999). Chemical and ionization efficiencies were determined using a combined ^{233}U–^{236}U–^{229}Th spike.

The VG-Sector™ TIMS instrument used is equipped with an 10 cm electrostatic filter and an ion-counting device. The abundance sensitivity of this device approximates 12 ppm as defined by Chen et al. (1992). The overall analytical reproducibility as estimated from replicate measurements of standard material, is usually better than $\pm 0.5\%$ for U concentration and $^{234}U/^{238}U$ ratios, and ranges from $\pm 0.5\%$ to 1% for $^{230}Th/^{234}U$ ratios (both ± 2 standard errors s_e). With the Altamira cave samples, the precision achieved for ^{230}Th measurements was much lower (± 5–13%). Low ^{230}Th concentrations, resulting from low U contents and young ages, and high ^{232}Th concentrations, due to the abundance of detrital particles, combined to make $^{230}Th/^{232}Th$ ratio measurements difficult. We had to process samples large enough to get ^{230}Th counts well above background. This led us to load at the same time high amounts of ^{232}Th, because of the "dirty samples". Unfortunately, the ionization efficiency of Th decreases with increasing amounts of Th loaded on the filament, as shown by Edwards et al. (1987). In addition, $^{232}Th/^{230}Th$ mass ratios over 180,000, in several samples, resulted in ^{230}Th counts indistinguishable from background level. This led us to run, in parallel, alpha-spectrometry measurements with an EGG-ORTEC™ instrument. We analyzed both calcite samples from layers A, B, C, H, and the clay fraction ($< 63\,\mu m$) from layers L and M. Chemical separation for U and Th was achieved as above, using ^{232}U and ^{228}Th as combined tracers to determine the chemical and counting efficiencies. Correction for the ^{228}Th-contribution from the decay of the sample ^{232}Th was made assuming secular equilibrium between the latter and its daughter ^{228}Th. After chemical separation and purification, the U and Th solutions were electrodeposited on steel discs. On a routine basis, the chemical yields for Th and U extractions averaged 50% and 35%, respectively. Spectral resolution was usually of the order of 65 KeV. The precision for $^{234}U/^{238}U$ ratio

measurements was generally better than $\pm 5\%$ (± 1 s). It ranged between 5% and 10% for $^{230}Th/^{232}Th$ ratios in the present study (± 1 s).

The chemical separation and spiking for MC-ICP-MS measurements was as for TIMS measurements above. Equipped with WARP (Wide Angle Retarding Potential), the MC-ICP-MS (isoprobe™) instrument has an abundance sensitivity of 100 ppb, i.e., thus allowing to determine 2 orders of magnitude $^{230}Th/^{232}Th$ mass ratios in comparison with TIMS. This feature is crucial when analysing ^{232}Th rich dirty samples. In addition, Th ionization with MC-ICP-MS is independent of the quantity of Th injected. These properties allow practically to inject if needed large quantities in order to obtain enough quantity of ^{230}Th. Nevertheless, for MC-ICP-MS the solutions were introduced by aspiration through a Teflon™ microprobe tubing and a glass expansion nebulizer. The system was cleaned for several minutes between sample runs with 4% HNO_3 followed by a rinse with 2% HNO_3. Baselines were measured above each peak at the beginning of each block (Hillaire-Marcel et al., 2000). The overall analytical reproducibility, as estimated from replicate measurements of standard compounds, is better than 2% for $^{234}U/^{238}U$ and $^{230}Th/^{234}U$ ratios.

Some corrections had to be made in order to calculate isochron ages for the "dirty" calcite analyzed here, in order to determine $^{230}Th/^{234}U$ and $^{234}U/^{238}U$ ratios in the fraction of U-series isotopes strictly linked to the fraction of U co-precipitated with calcite, in contrast to the fraction inherited from the detrital particles incorporated into the calcite. Henceforth, we will refer to the first of these fractions as to the "authigenic fraction" (i.e., linked to calcite deposition), and to the second, as to the "detrital fraction". The $^{234}U/^{238}U$ and $^{230}Th/^{234}U$ ratios of the "authigenic fraction" were calculated using Rosholt isochron plots: $^{230}Th/^{232}Th$ vs. $^{234}U/^{232}Th$ and $^{234}U/^{232}Th$ vs. $^{238}U/^{232}Th$ (Rosholt, 1976; Kaufman, 1993).

2.3. Radium analyses

Radium analyses were performed on ~ 1.5 g of powdered sample. As for U-Th analyses, we used total sample dissolution. Chemical separation involved a three-stage procedure. Ra and Ba were extracted using the cation exchange resin Biorad™ AG 50W-X8 in 10 ml columns using 5N HNO_3, and subsequently using 6N HCl (loaded in 3N HCl each time). Thereafter, Ra was separated from Ba on a Sr-Spec™ resin in 1 ml columns with 3N HNO_3. Finally, Ra-purification was achieved using a True Spec™ resin in 0.5 ml columns with 2N HNO_3 (modified from Chabaud et al., 1994). The measurements were performed on a VG-Sector 54™ mass spectrometer equipped with a Daly ion-counting detector. Because of the low radium content of the samples (5 femtograms), a low-background ion-counting system as well as good chemical blanks were essential. The system used here had a reproducible background of 4 cps, whereas blanks were under detection limits. The overall analytical reproducibility, as estimated from replicate measurements of standards, was better than $\pm 0.5\%$.

The concentrations and activity ratios of U–Th series isotopes in calcitic layers and clayey layers, are listed in Table 1, and are all quoted with their ± 2 s error.

2.4. AMS-^{14}C measurements

Aliquots for ^{14}C measurements by AMS were recovered from 10 of the samples used for U and Th series measurements, above. The analyses were performed at the IsoTrace laboratory of the University of Toronto (Canada). The results are corrected for natural and sputtering fractionation to a base of $\delta^{13}C = -25‰$, and errors are given at $\pm 1\sigma$ level (Table 2).

3. Results

3.1. ^{14}C ages

The conventional ^{14}C ages obtained range from 10.7 ka (top layer) to 12.9 ka (bottom layer) (Table 2). They correspond to calibrated ages ranging between $12{,}858 \pm 70$ and $15{,}510 \pm 350$ BP, respectively. These ages are slightly younger than those obtained on archaeological material from the cave (e.g., Almagro and Fernandez-Miranda, 1978). They would not be incompatible with a Bölling-Alleröd age for the deposition of the flowstone, or a younger age, depending on the ^{14}C activity of dissolved carbon in the cave.

3.2. Stable isotope records

In order to determine the appropriateness of using stable isotopic records for paleohydrological-paleoclimate reconstructions, the pre-requisite of calcite precipitation in isotopic equilibrium with ambient waters must be ascertained. This usually requires low CO_2 release rates during calcite precipitation. This is often the case in poorly ventilated caves (e.g., Bar-Matthews et al., 1996; Desmarcheliers et al., 2000). Altamira cave is likely to have fallen into this category after the collapse of its roof that resulted in the closure of its entrance. A couple of isotopic criteria are commonly used to assess isotopic equilibrium conditions (Hendy, 1971): $\delta^{18}O$ values should remain constant along a given single growth layer, and there should not be any correlation between $\delta^{18}O$ and $\delta^{13}C$ values along such a layer.

Table 1
U–Th–Ra measurements in the calcitic layers and clayey layers[a]

Samples	Depth (cm)	Analyse	U (ppb)	^{238}U (dpm/g)	Th (ppb)	^{232}Th (dpm/g)	^{230}Th (dpm/g)	^{226}Ra (dpm/g)	(^{234}U/^{238}U)	(^{230}Th/^{232}Th)
Calcite fraction										
A-top B	0.3–1	TIMS	39.09±0.18	0.02917±0.00013	18.24±0.32	0.004486±0.000078	0.00530±0.00040		1.104±0.011	1.181±0.87
A-top	1–3	*TIMS*	*51.55±0.20*	*0.03856±0.00015*	*13.52±0.32*	*0.003326±0.000078*	nd		*1.109±0.012*	nd
A-top bis	0.7–3	TIMS	52.50±0.30	0.03917±0.00023	10.65±0.13	0.002619±0.000031	0.00595±0.00042		1.151±0.021	2.27±0.16
A-12	4–6	*Alpha*	*44.8±2.4*	*0.0334±0.0018*	*16.3±3.3*	*0.0040±0.0008*	*0.006±0.001*	*0.0058±0.0003*	*1.18±0.096*	*1.5±0.4*
A-12	4–6	MC-ICP-MS	39.40±0.79	0.02940±0.00059	15.80±0.32	0.003887±0.000078	0.00574±0.00011	0.0055±0.0001	1.190±0.024	1.478±0.030
B-top	7.6–8.5	TIMS	43.32±0.20	0.03232±0.00015	62.2±1.2	0.01531±0.00029	0.0119±0.0015		1.156±0.014	0.775±0.098
B-12	10–11.5	*Alpha*	*60.0±2.9*	*0.0448±0.0022*	*39.8±4.9*	*0.0098±0.0012*	*0.0104±0.0012*		*1.147±0.040*	*1.06±0.09*
B-12	10–11.5	MC-ICP-MS	45.76±0.92	0.03414±0.00068	28.83±0.58	0.00709±0.00014	0.00771±0.00015		1.125±0.023	1.087±0.022
B-bottom bis	12–13	*TIMS*	*49.59±0.14*	*0.03700±0.00011*	*24.08±0.22*	*0.005924±0.000055*	nd		*1.104±0.010*	nd
B-11	13.5–14.7	*Alpha*	*48.8±3.2*	*0.0364±0.0024*	*39.8±3.3*	*0.0098±0.0008*	nd		*1.03±0.18*	nd
C-top bis	16.7–18.7	*TIMS*	*41.01±0.11*	*0.03060±0.00008*	*17.05±0.15*	*0.004194±0.000038*	nd		*1.10±0.01*	nd
C-10	20.7–22	*TIMS*	*40.31±0.21*	*0.03007±0.00015*	*31.75±0.71*	*0.00781±0.00018*	nd		*1.124±0.016*	nd
C-11	22.7–23.7	Alpha	33.8±3.2	0.0252±0.0024	41.1±2.4	0.0101±0.0006	0.0109±0.0006		1.10±0.14	1.08±0.10
C-bottom	24.2–26.2	*TIMS*	*40.38±0.13*	*0.03013±0.00009*	*18.36±0.36*	*0.004515±0.000088*	nd		*1.121±0.012*	nd
C-bottom	24.2–26.2	Alpha	78.4±4.6	0.0585±0.0034	166.3±6.5	0.0409±0.0016	0.0337±0.0014		0.97±0.16	0.824±0.046
H-11	44.2–46.2	*Alpha*	*49.0±4.2*	*0.0366±00.0031*	*30.5±5.2*	*0.0075±0.0013*	nd		*1.10±0.12*	nd
H-top bis	47.2–48.7	*TIMS*	*49.93±0.16*	*0.03725±0.00012*	*18.05±0.14*	*0.004441±0.000035*	nd		*1.111±0.010*	nd
H middle	49.7–51.2	Alpha	55.4±2.9	0.0413±0.0022	15.0±1.6	0.0037±0.0004	0.0092±0.0008		1.25±0.10	2.49±0.40
H-12	50–51.7	*Alpha*	*63.9±2.9*	*0.0477±0.0022*	*20.3±3.3*	*0.0050±0.0008*	*0.0081±0.0010*		*1.046±0.66*	*1.62±0.32*
H-12	50–51.7	MC-ICP-MS	50.8±1.0	0.03791±0.00076	16.73±0.33	0.004115±0.000082	0.00749±0.00015		1.101±0.022	1.821±0.036
H-10	49.8–51.5	TIMS	54.02±0.30	0.04030±0.00022	17.16±0.29	0.004222±0.000071	0.00936±0.00082		1.123±0.014	2.22±0.19
H-bottom	52–53.2	TIMS	54.64±0.32	0.04076±0.00024	17.54±0.14	0.004315±0.000035	0.00850±0.00024		1.118±0.010	1.970±0.054
Clayey fraction (<63 μm)										
L		Alpha	553±34	0.413±0.025	3138±156	0.772±0.038	0.455±0.029		0.839±0.039	0.589±0.048
M		Alpha	472±23	0.3522±0.0172	2745±106	0.675±0.026	0.409±0.020		1.011±0.035	0.606±0.038

[a] Nd: not determined. Data in italic are not used for isochron age determination because: (i) ^{230}Th analyse was not determined or not precise enough or, (ii) both alpha spectrometry and MC-ICP-MS measurements were performed on these samples and MC-ICP-MS data were prefered.

Table 2
Comparison between ^{14}C and U/Th ages

Sample	Depth (cm)	^{14}C Age (ka) Uncalibrated BP	^{14}C Age (ka) Calibrated BP	U/Th Isochron	
				Analyse	Age (ka)
A-Top B	0.3–1	10.70±0.08	12.85±0.07	TIMS	11.8±0.8
A-Top bis	0.7–3	—	—	TIMS	
A-12	4–6	10.93±0.09	12.95±0.08	MC-ICP-MS	
B-top	7.6–8.5	10.89±0.09	12.93±0.09	TIMS	11.9±1.8
B-12	10–11.5	—	—	MC-ICP-MS	
C-11	22.7–23.7	12.40±0.13	14.54±0.41	Alpha	22±3
C-bottom	24.2–26.2	12.20±0.08	14.21±0.14	Alpha	
H-middle	49.7–51.2	12.70±0.08	14.97±0.60	Alpha	21±2
H-10	49.8–51.5	—	—	TIMS	
H-12	50–51.5	12.48±0.10	14.50±0.32	MC-ICP-MS	
H-bottom	52–53.2	12.90±0.08	15.51±0.35	TIMS	

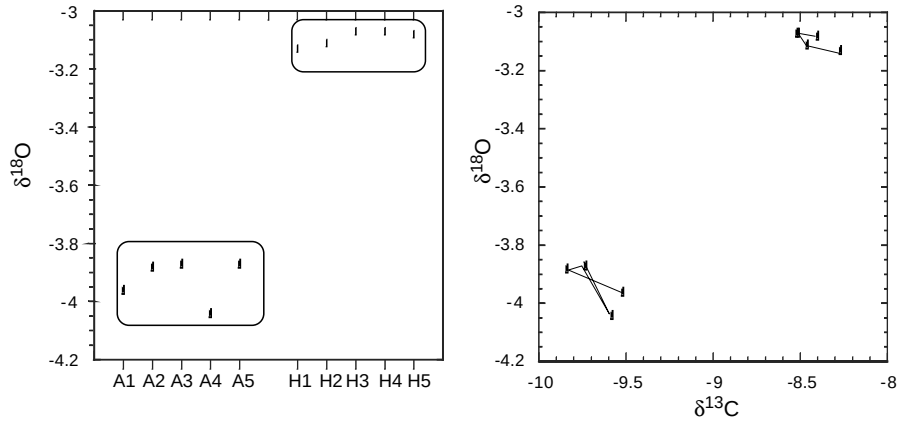

Fig. 2. Hendy's tests for growth layers in the studied flowstone. Left: near constant $\delta^{18}O$ values along growth layers from units A and H. Right: uncorrelated $\delta^{18}O$ vs. $\delta^{13}C$ values along single growth layers from units A and H.

Tests were made using the A and H layers. $\delta^{18}O$ values vary by not more than 0.2‰ and 0.1‰, respectively, along these layers (Fig. 2). They also depict uncorrelated $\delta^{18}O$ and $\delta^{13}C$ values, indicating that no significant kinetic effects occurred during carbonate precipitation (Fig. 2). One may thus assume isotopic equilibrium conditions during the deposition of the flowstone.

The oxygen isotope profile (Fig. 3) depicts very small fluctuations between a maximum value of approximately −2.9‰ (bottom of layer C) and a minimum value of ∼−3.8‰ (top of layer A), leading to the conclusion that the flowstone formed during a period showing relatively stable climate conditions. This is confirmed by the fact that $\delta^{13}C$ values, often tightly dependent upon hydrological conditions in the soils of the groundwater recharge area (Dulinski and Rozanski, 1990; Baker et al., 1997), show negligible fluctuations within a narrow range (−8.8±0.5‰; Fig. 3).

3.3. U and Th series isotope data

Uranium concentrations are relatively constant, but low when compared to other cave deposits where the concentration range is generally 2–0.05 ppm (Latham et al., 1986; Gascoyne, 1992; Lauritzen, 1995; Kaufman et al., 1998; Rihs et al., 1999; Hellstrom and McCulloch, 2000). ^{238}U concentrations range from 30 to 78 ppb. In contrast, ^{232}Th concentrations vary more widely between 11 and 160 ppb (Fig. 3; Table 1). They indicate the presence of variable amounts of detrital particles in the flowstone and could be considered as an important content of detrital material due to the young age of the samples and their relatively low U content.

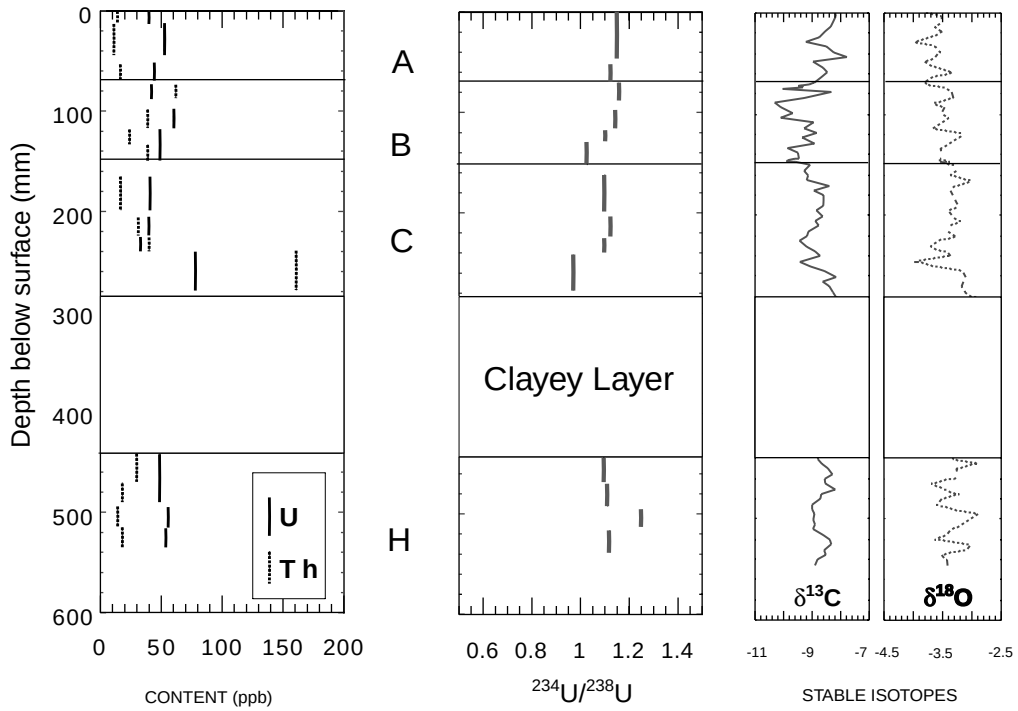

Fig. 3. U and Th concentrations (in ppb), $^{234}U/^{238}U$ activity ratio and stable isotope composition (in ‰ vs. V-PDB) of the flowstone sequence. The black square on top of the $\delta^{18}O$ profile corresponds to equilibrium conditions under modern condition.

Table 3
$^{230}Th/^{234}U$ and $^{234}U/^{238}U$ ratios of the "authigenic" fraction vs. $^{230}Th/^{232}Th$ ratios in the "detrital" component from isochrons of Fig. 4

Layers	$^{230}Th/^{234}U$ Authigenic component	$^{234}U/^{238}U$ Authigenic component	$^{230}Th/^{232}Th$ detrital component	Age (ky)
Layer A	0.103 ± 0.006	1.186 ± 0.018	0.583 ± 0.073	11.8 ± 0.8
Layer B	0.104 ± 0.015	1.101 ± 0.003	0.579 ± 0.097	11.9 ± 1.8
Layer C	0.185 ± 0.020	1.274 ± 0.038	0.698 ± 0.037	22 ± 3
Layer H	0.179 ± 0.013	1.813 ± 0.094	<0	21 ± 2

Plotted as Rosholt diagrams, samples from layers A and B yield highly correlated linear trends, allowing to calculate precise $^{230}Th/^{234}U$ activity ratios for the "authigenic fraction". They average 0.103 ± 0.006 and 0.104 ± 0.015 in layers A and B, respectively (Table 3; Fig. 4). The corresponding $^{234}U/^{238}U$ activity ratios are 1.186 ± 0.008 and 1.101 ± 0.003, respectively (Table 3). This allows the calculation of isochron ages of $11{,}820 \pm 800$ and $11{,}900 \pm 1800$ for the corresponding layers (the errors on the slopes and ages were calculated at ± 2 s uncertainty using the *Isoplot* software).

Data from layers C, just above the clay-rich layer, yielded very close points due to the presence of an abundant detrital fraction (as depicted by ^{232}Th concentrations in sample C; Table 1) and cannot provide reliable isochron age. Data from layer H, just below the clay-rich layer, indicate scattered data points with Rosholt isochron plots due to the heterogeneity of the isotopic composition of this fraction (see below).

Radium measurements in layer A, were used to calculate $^{226}Ra/^{230}Th$ activity ratios of 0.96 ± 0.05 with ^{230}Th measurement obtained by MC-ICP-MS, based on MC ICP-MS measurements of the ^{230}Th concentrations (Table 1). This value corresponds to an apparent age of 20,800 years for the $^{226}Ra/^{238}U$ system (see Section 4.2).

4. Discussion

4.1. U/Th isochron ages vs. isotopic heterogeneities in the detrital fraction

The basic assumptions, when using Rosholt isochron plots, are (i) that the "authigenic" U and its daughter ^{230}Th behave as dilutants of an homogeneous "detrital"

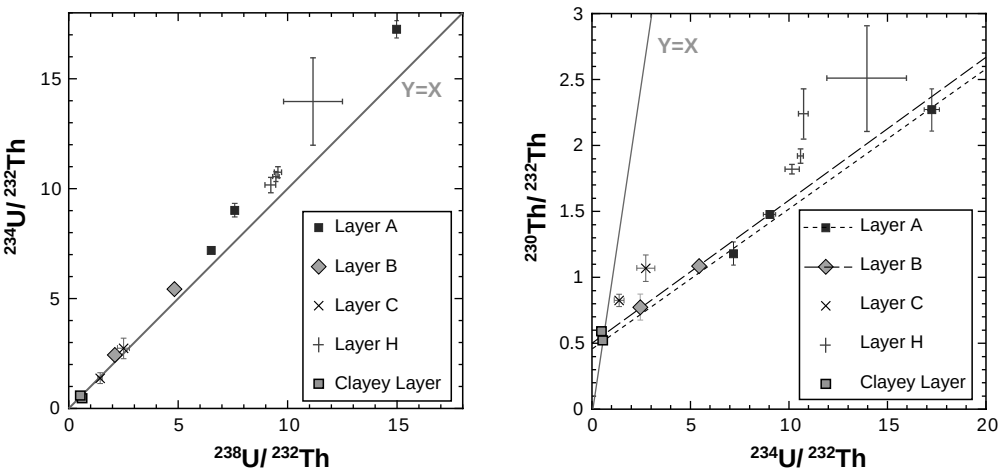

Fig. 4. Rosholt's isochrons for layers A, B, C, H.

component (i.e., a component characterized by uniform U/^{232}Th and ^{230}Th/^{232}Th ratios; see a discussion in Hillaire-Marcel et al., 1995), and (ii) that the system maintained chemically closed since deposition of the "authigenic" component. In Rosholt isochrons [^{230}Th/^{232}Th vs. ^{234}U/^{232}Th and ^{234}U/^{232}Th vs. ^{238}U/^{232}Th], the detrital component could show a slight excess of ^{230}Th vs. its parent U (see discussion in Bischoff and Fitzpatrick, 1991) due to U leaching in soil processes. In situation when ^{234}U/^{238}U activity ratios are not much different from secular equilibrium as it is the case here (see Table 1), the intercept between the sample regression lines and the $X = Y$ lines (equipoint) provides a good estimate for the ^{230}Th/^{232}Th ratio in the detrital endmember (see discussion in Bischoff and Fitzpatrick, 1991). Here, equipoint values of ^{230}Th/^{232}Th ratios of 0.583 ± 0.073 and 0.579 ± 0.097 are obtained in layers A and B, respectively. They are almost identical to the ratios in the detrital layers L + M. Therefore, we are led to conclude that the detrital fraction remained unchanged, from an isotopic view point, during the deposition of the A–B flowstone layer, and that this deposition occurred during a very short time interval. Considering the isotopic homogeneity of the "detrital" endmember and the identity of both isochron slopes (Fig. 4), the corresponding isochron age (11.8 ± 0.8; Table 3) seems a robust estimate for the deposition age of the uppermost flowstone unit.

For layers A and B, the authigenic fraction represents an average of approximately 90% of the uranium present, based on the estimate from the equipoint ratios (see above) and U/Th ratios in layers A and B. This yields a very low U/Ca mass ratio during precipitation (about 10^{-7}), although not unusual in speleothem calcites (e.g., Gascoyne et al., 1978)

Data sets for layer H, below, seem to indicate a real lack of homogeneity in the isotopic composition of the detrital fraction. In addition, semi-quantitative estimates of calcite abundance by X-ray diffraction show that the fine fraction ($< 63\,\mu m$) in layers L and M is composed of 80–88% of calcite, and thus that it is composed of a mixture of clay and calcite, either of detrital or authigenic origin. Thus, differences in the isotopic composition of the detrital fractions in the more heterogeneous layers underlying units A and B, may be due to variable grain size distributions or calcite/clay ratios between their respective detrital fractions. Lithologic variations in detrital supplies could be linked to changes in the hydrologic flow in the cave and/or in soil conditions and climate during recharge.

4.2. Radium-226

The total ^{226}Ra present in a given sample includes three fractions. One $(^{226}\mathrm{Ra})_{\mathrm{detrital}}$ is carried by the detrital fraction incorporated into the sample. A second one $(^{226}\mathrm{Ra})_{\mathrm{authigenic}}$ originates from the decay of the "authigenic" uranium co-precipitated with the calcite. A third one, $(^{226}\mathrm{Ra})_{\mathrm{excess}}$, represents the residuals of the ^{226}Ra initially present in groundwater's and co-precipitated with calcite. The isotopic signature of the detrital endmember, as estimated above from the intercept between the isochron line and the $Y = X$ line, provides a direct estimate for the first fraction $(^{226}\mathrm{Ra})_{\mathrm{detrital}}$. We assume that ^{226}Ra, ^{230}Th and ^{234}U from detrital particles are in secular equilibrium. Then, the ^{226}Ra activity of this fraction may be simply derived from the ^{232}Th activity of the sample:

$$(^{226}\mathrm{Ra})_{\mathrm{detrital}} \approx (^{230}\mathrm{Th}/^{232}\mathrm{Th})_{\mathrm{intercept}} \times (^{232}\mathrm{Th})_{\mathrm{activity}}$$

The second fraction of the total ^{226}Ra, i.e. that produced by the "authigenic" uranium, builts up with the growth of the intermediate ^{230}Th. The ^{230}Th-isochron age, as calculated above, is thus used to calculate this

$(^{226}Ra)_{authigenic}$ fraction:

$$(^{226}Ra/^{238}U)_{authigenic} = 1 + \frac{\lambda_{Th}}{\lambda_{Ra} - \lambda_{Th}} e^{(-\lambda_{Ra} \times t)} - \frac{\lambda_{Ra}}{\lambda_{Ra} - \lambda_{Th}} e^{(-\lambda_{Th} \times t)} + ((^{234}U/^{238}U) - 1) \times \left[\frac{\lambda_{Ra}\lambda_{Th}}{(\lambda_U - \lambda_{Th})(\lambda_U - \lambda_{Ra})} + \frac{\lambda_{Ra}\lambda_{Th} e^{(-(\lambda_{Th} - \lambda_U) \times t)}}{(\lambda_{Th} - \lambda_U)(\lambda_{Th} - \lambda_{Ra})} + \frac{\lambda_{Ra}\lambda_{Th} e^{(-(\lambda_{Ra} - \lambda_{Th}) - \times t)}}{(\lambda_{Ra} - \lambda_U)(\lambda_{Ra} - \lambda_{Th})} \right],$$

where λ are the decay constant of $\lambda_{Ra} = \lambda_{226_{Ra}}, \lambda_{Th} = \lambda_{230_{Th}}, \lambda_U = \lambda_{234_U}$.

At the time scale of ^{226}Ra decay, one may assume a constant $^{234}U/^{238}U$ activity ratio, i.e., a negligible weight loss of the parent ^{234}U. Then, using the ^{230}Th-isochron age of 11.8 ± 0.8 to carry on the daughter ^{226}Ra activity of the "authigenic" U to its present value, we obtain $2.75 \times 10^{-3} \pm 1.19 \times 10^{-3}$ dpm/g for this second ^{226}Ra fraction.

Subtracting the above two fractions from the total radium-226 activity, one obtains the residual $^{226}Ra_{excess}$ value: $7.89 \times 10^{-3} \pm 1.27 \times 10^{-3}$ dpm/g. The isochron age of 11.8 ± 0.8 ka is used to return to the corresponding initial $^{226}Ra_{excess}$ value, as follows:

$$[^{226}Ra_{excess}]_0 = [^{226}Ra_{excess}]_{Residual} \times e^{\lambda_{Ra} \times t} = 0.123 \pm 0.046 \text{ dpm/g}.$$

When comparing this activity to that of the "authigenic" uranium as estimated above, one obtains a $^{226}Ra/^{238}U$ activity ratio of ~ 4.5 for the co-precipitated component, suggesting a major fractionation process between these two isotopes, either in soils, during groundwater recharge, or later on during the underground circulation of the water. Since uranium is a redox sensitive element, in contrary to radium, reduced conditions likely induced U-retention somewhere in the hydrogeological pathway, upstream.

4.3. ^{14}C dating

The use of ^{14}C ages requires the estimation of the dead carbon proportion, due to limestone dissolution or to soil organic matter oxidation (Genty and Massault, 1997; Genty et al., 1999). Here, a comparison of the normalized ^{14}C ages (T_{14_C}) in layers A and B (mean value: 10.9 ± 0.1, i.e., $\pm 1\sigma$) with the corresponding ^{230}Th-isochron age ($T_{isochron}$; here 11.8 ± 0.4 ka, i.e., $\pm 1\sigma$), may allow an estimate of the initial (isotopically normalized) deficit or excess in ^{14}C of the cave DIC ($\Delta_1^{14}C$) and the atmospheric CO_2 ($\Delta_2^{14}C$) at the time of deposition of these layers as follows:

$$\Delta^{14}C(‰) = 10^3 \times (\exp(\lambda_{14_{C_{Real}}} T_{isochron} - \lambda_{14_{C_{Libby}}} T_{14_C}) - 1)$$

with $\lambda_{14_{C_{Real}}}$ standing for the radioactive decay constant of ^{14}C, and $\lambda_{14_{C_{Libby}}}$ standing for the constant of Libby.

Here, we obtain a value of $\Delta_1^{14}C = 73 \pm 50‰$ ($\pm 1\sigma$). This value must be compared to the (normalized) ^{14}C activity of the atmospheric CO_2 of the period which may be obtained from current ^{14}C-calibration software. We used here INTCAL 98 (from Stuiver et al., 1998). The isochron age of 11.8 ± 0.4 ($\pm 1\sigma$) corresponds to an uncalibrated ^{14}C age of 10.65 ± 0.20 ka, thus to an initial $\Delta_2^{14}C$ value of $\approx 100 \pm 60‰$ for the atmospheric CO_2. Accordingly, the difference in (normalized) ^{14}C activity between the cave CO_2 and the atmospheric CO_2 of that period can be estimated to be $\approx 30 \pm 80‰$ ($\pm 1\sigma$). It is concluded that, within standard deviation, the cave CO_2 was in equilibrium or near equilibrium with the atmosphere during the final deposition of the flowstone layer. It seems highly probable that the same situation prevailed since the human occupation of the cave, i.e., when a higher ventilation rate of the cave can be inferred, and therefore that the calibrated ^{14}C ages (Table 2) of the layers deposited prior to units A and B above, likely provide the best age estimates for the depositional age of these lower units of the flowstone.

The relatively large uncertainties in the calculation of the $\Delta^{14}C$ values above are not very significant since the sets of ages of the flowstone partly fall into the ^{14}C plateau interval of the Younger Dryas (Becker and Kromer, 1993). As explained below, isotopic paleohydrologic interpretation can be used to constrain the climatic and temporal frame of the final flowstone depositional interval, with respect to the cold climate conditions and the age of the Younger Dryas.

4.4. Isotopic paleohydrology

Under present day conditions, the mean annual temperature (MAT) of the Altamira area is 14°C. Using Dansgaard's relationship between MAT and $\delta^{18}O$ in precipitation (Dansgaard, 1964) and the carbonate paleotemperature equation of Epstein et al. (1953), one may calculate a first order estimate for the isotopic composition of a calcite that would precipitate today under equilibrium conditions ($\delta^{18}O$-$CaCO_3$-eq. $\sim -3.2‰$). It will be used as a benchmark value to compare with past conditions.

In the upper flowstone unit, $\delta^{18}O$ values decrease from $-2.9‰$ at the base of layer C to $-3.8‰$ at the top of layer A (Fig. 5). Taking into account the fact that the oceanic source of atmospheric moisture was slightly heavier during this period than it is today (by approximately 0.4–0.5‰; see Shackleton, 1987), the observed calcite-$\delta^{18}O$ values suggest a slightly colder climate during the precipitation interval, than today. The observed carbonate $\delta^{18}O$ value suggest a slightly colder climate (-1°C or -2°C) during the precipitation interval than today. During the precipitation interval, the shift in the estimated air temperature towards minimum values (Fig. 5) correspond to the deposition

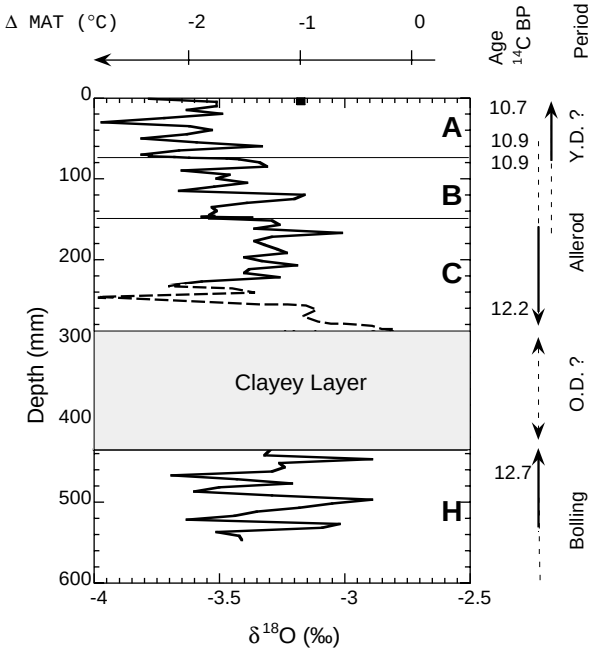

Fig. 5. Shift in precipitation temperature suggested by stable oxygen isotope data. The black square represents modern conditions. The dashed line corresponds to interval with correlated $\delta^{18}O$ and $\delta^{13}C$ shifts. Thus, to period where cinetics effects occurs during calcite precipitation. Δ MAT is vs. modern conditions, see text.

of layers A and B. It seems that this occurs during a very short period of time since layers A and B yield similar age in standard deviation. This drop in temperature has probably provoked a drastic change of the vegetation (Penalba et al., 1997) and an interruption of the deposition above layers A and B. Temperatures during the Younger Dryas were estimated to be 8°C cooler than today in the area (Duplessy et al., 1993; Penalba et al., 1997). If this interpretation is valid, then the onset of the Younger Dryas event precisely dates here at 11.8 ± 0.8 ka ($\pm 2\sigma$) on a calendar time scale.

Based on the ^{14}C age frame (Fig. 5), the flowstone depositional interval should encompass the Older Dryas event. The clayey layer, between units H and C, could represent this interval. However, the stable isotope record does not suggest any significant change in climate at the upper and lower boundaries of this layer. Thus, the Older Dryas might well have been too discrete here to be recorded. Worthy of mention is the fact that terrestrial paleoclimate records from the area also do not indicate significant climate changes during the Older Dryas (e.g., Penalba et al., 1997).

4.5. Linkage of ^{14}C and ^{230}Th chronologies of the interval

The age for the onset of the Younger Dryas obtained here could be compared with other time series from nearby sites. Inland, these include notably a record of Mg/Ca ratio changes in ostracods from La Draga sequence (Lake Banyoles, NE Spain; Wansard, 1996) and the Quintanar de la Sierra pollen sequence (Sierra de Neila, N Spain; Penalba et al., 1997). A nearby North Atlantic core (SU81-18; 37°46′N, 10°11′W), located off Portugal (Bard et al., 1987; Duplessy et al., 1993), could also be used for reference.

The ^{230}Th-isochron age (11.8 ± 0.8 ka, 2σ) suggests a slightly younger age for the onset of the Younger Dryas, at the study site, than currently cited elsewhere based on calibrated ^{14}C ages. The onset of the Younger Dryas is set at ≈12,960 cal. years B.P. in the GISP2 ice core record (Alley et al., 1993), at ≈12,700 cal. years B.P. in the GRIP record (Johnsen et al., 1992), at ≈10,650 ^{14}C B.P. (≈12,885 cal. years B.P.), in the pollen sequence of Quintanar de la Sierra, and at ≈10,640 ^{14}C BP (≈12,750 cal. years BP), in the SU81-18 record. On the contrary, U–Th data from La Draga sequence, yielded an age of ≈11,900 years, compatible with our data set.

The ~1 ka difference between the calibrated ^{14}C ages and the ^{230}Th ages for the onset of the Younger Dryas, suggests either that (i) the Younger Dryas episode could encompass a series of climate events that were not in phase, or (ii) that the calibration of the ^{14}C time scale at the onset of the Younger Dryas is still not well constrained (see Bard et al., 1990; Edwards et al., 1993), or (iii) that our isochron age and the ^{230}Th age of la Draga sequence are wrong. However, we are led to put some credit on the isochron age obtained here for two reasons. Firstly, we have no geochemical indication for a post-depositional gain in U that could account for an age younger than expected, in addition to the fact that such a secondary fixation of U would be highly improbable here in view of the low porosity of the flowstone layer. Secondly, variable contamination effects due to heterogeneities in detrital particles would more likely have resulted in a ^{230}Th-isochron slope higher than that corresponding to the 11.8 ± 0.8 ka isochron age. For instance, such "aging" effects are clearly shown by the data sets from the lower unit H.

5. Conclusion

Paradoxically, in the present study, ^{14}C ages are shown to yield the best age estimates for the deposition of the Altamira cave flowstone post-dating the Magdalenian occupation of the cave. However, this conclusion would have been impossible based only on ^{14}C measurements alone. Indeed, allowing for some ^{14}C depletion in the cave CO_2 and DIC, during calcite deposition, the set of apparent ^{14}C ages obtained (i.e., 10–13 ka), would not have been incompatible with a precipitation episode occurring during the early Holocene, for example. Complementary isotopic information helped to discard such a possibility. It includes notably:

(i) near secular equilibrium conditions between ^{226}Ra and ^{230}Th, suggesting a depositional age >8 ka (i.e., ~ 5 half-lifes of ^{226}Ra); (ii) ^{230}Th/^{232}Th vs. ^{234}U/^{232}Th isochron age in the upper crust (A + B) of 12 ka, and (iii) oxygen isotope data suggesting precipitation under climatic conditions compatible with a pre-Younger Dryas age assignment. The array of isotopic data lead to validation of the ^{14}C ages for the precipitation episode. The base of the flowstone is dated at $15{,}500 \pm 300$ cal BP years (an age consistent with the archaeological frame here), and its top at $\sim 11.8 \pm 0.8$, at the onset of the Younger Dryas. The flowstone deposition thus occurred during the Bölling–Alleröd period.

Acknowledgements

We acknowledge the two anonymous reviewers. We thank Dr. M. Hoyos (Museo nacional de Ciencias naturales, Madrid) and Dra. C. Zazo (CSICyT, Madrid) for their help in the course of the present study. We mention particularly the collaboration of Dr. Hoyos that was essential for the field study and sampling program in the cave. Unfortunately, Dr. Hoyos passed away before he could participate in the writing of the present paper. We also owe thanks to the director of the Altamira cave, Mr V. Cabrera Valdés, who provided access and advice to conduct the sampling program in the protected site of Altamira. Finally, Sergio Sabchez, Juan-Carlos Canaveras (Museo nacional de Ciencas naturales, Madrid) and Dr. Christine Veiga-Pires (University of Algarve, Portugal) were very helpful during the sampling program in the field, Drs. Deke Cheng and Guy Bilodeau (GEOTOP-UQAM) provided critical help for stable isotope analyses, Pierre Deschamps provided useful comments on the U/Th and Ra data interpretations, and Dr. R. Stevenson (GEOTOP-UQAM) made useful comments on an earlier version of the manuscript.

References

Alley, R.B., Meese, D.A., Shuman, C.A., Gow, A.J., Taylor, K.C., Grootes, P.M., Wuite, J.W.C., Ram, M., Waddington, E.D., Mayewski, P.A., Zielinski, G.A., 1993. Abrupt increase in Greeland snow accumulation at the end of the Younger Dryas event. Nature 362, 527–529.

Almagro, M., Fernandez-Miranda, M. (Eds.), 1978. Editors. C-14 y la prehistoria de la peninsula iberica. Madrid, Fundacion Juan Arce.

Baker, A., Ito, E., Smart, P.L., McEwan, R.F., 1997. Elevated values of ^{13}C in speleothems in a British cave system. Chemical Geology 136, 263–270.

Bard, E., Arnold, M., Duprat, J., Moyes, J., Duplessy, J.C., 1987. Retreat velocity of the North Atlantic polar front during the last deglaciation determined bu ^{14}C accelerator mass spectrometry. Nature 328, 791–794.

Bard, E., Hamelin, B., Fairbanks, R.G., Zindler, A., 1990. Calibration of the ^{14}C timescale over the past 30,000 years using mass spectrometric U-th ages from Barbados corals. Nature 345, 405–410.

Bar-Matthews, M., Ayalon, A., Mattews, A., Sass, E., Halicz, L., 1996. Carbon and oxygen isotope study of the active water–carbonate system in akarstic Mediterranean cave: Implications for paleoclimate research in Semiarid regions. Geochimica et Cosmochimica Acta 60, 337–347.

Becker, B., Kromer, B., 1993. The continental tree-ring record-absolute chronology, ^{14}C calibration and climatic change at 11 ka. Palaeogeography, Palaeoclimatology, Palaeoecology 103, 67–71.

Bischoff, J.L., Fitzpatrick, J.A., 1991. U-series dating of impure carbonates: An isochron technique using total-sample dissolution. Geochimica et Cosmochimica Acta 55, 543–554.

Carter, H.E., Warwick, P., Cobb, J., Longworth, G., 1999. Determination of uranium and thorium in geological materials using extraction chromatography. The Analyst 124, 271–274.

Chabaud, F., Ben-Othman, D., Birck, J.L., 1994. A new Ra-Ba chromatographic separation and its application to Ra mass-spectrometric measurement in volcanic rocks. Chemical Geology 114, 191–197.

Chen, J.H., Edwards, R.L., Wasserburg, G.J., 1992. Mass spectrometry and applications to uranium-series disequilibrium. In: Ivanovitch, M., Harmon, R.S. (Eds.), Uranium-Series Disequilibrium: Applications to Earth, Marine and Environmental Sciences. Clarendon press, Oxford (Chapter 6).

Conkey, M.G., 1980. The identification of prehistoric hunter-gatherer aggregation sites: the case of Altamira. Current Anthropology 21, 609–630.

Coplen, T.B., 1995. Discontinuance of SMOW and PDB. Nature 375, 285–288.

Dansgaard, W., 1964. Stable isotopes in precipitations. Tellus 16, 436.

Desmarcheliers, J.M., Goede, A., Ayliffe, L.K., McCulloch, M.T., Moriarty, K., 2000. Stable isotope record and its paleoenvironmental interpretation for a late middle Pleistocene speleothem from Victoria Fossil Cave, Naracoorte, South Australia. Quaternary Science Reviews 19, 763–774.

Dorale, J.A., Edwards, R.L., Ito, E., Gonzales, L.A., 1998. Climate and vegetation history of the midcontinent from 75 to 25 ka: A speleothem record from Crevice Cave, Missouri, USA. Science 282, 1871–1874.

Dorale, J.A., Gonzales, L.A., Reagan, M.K., Pickett, D.A., Murrell, M.T., Baker, R.G., 1992. A high resolution record of Holocene climate change in speleothem calcite from cold water cave, northeast Iowa. Science 258, 1626–1630.

Dulinski, M., Rozanski, K., 1990. Formation of ^{13}C/^{12}C isotope ratios in speleothems, a semi-dynamic model. Radiocarbon 32, 7–16.

Duplessy, J.C., Bard, E., Labeyrie, L., Duprat, J., Moyes, J., 1993. Oxygen isotope records and salinity changes in the Northeastern Atlantic Ocean during the last 18,000 years. Paleoceonography 8, 341–350.

Edwards, R.L., Chen, J.H., Wasserburg, G.J., 1987. ^{238}U–^{234}U–^{230}Th–^{232}Th systematics and the precise measurement of time over the past 50,000 years. Earth and Planetary Science Letters 81, 175–192.

Edwards, R.L., Beck, J.W., Burr, G.S., Donahue, D.J., Chappell, J.M.A., Bloom, A.L., Druffel, E.R.M., Taylor, F.W., 1993. A large drop in atmospheric ^{14}C/^{12}C and reduced melting in the Younger Dryas, documented with ^{230}Th ages of corals. Science 260, 962–968.

Epstein, S., Buchsbaum, R., Lowenstam, H., Urey, H.C., 1953. Revised carbonate–water isotopic temperature scale. Bulletin of the Geological Society of America 64, 1315.

Gascoyne, M., 1992. Palaeoclimate determination from cave calcite deposits. Quaternary Science Reviews 11, 609–632.

Gascoyne, M., Schwarcz, H.P., Ford, D.C., 1978. Uranium series dating and stable isotope studies of speleothems: Part I theory and techniques. British Cave Research Association 5, 91–111.

Gewelt, M., 1986. Datation ^{14}C des concrétions de grottes belges: vitesses de croissance durant l'holocène et implications paléoclimatiques. In: Patterson, K., Sweeting, M.M. (Eds.), New Directions in Karst, Proceedings of the Anglo-French Karst Symposium, September 1983. GEO Books, Norwich, pp. 293–322.

Genty, D., Massault, M., 1997. Bomb ^{14}C recorded in laminated speleothems: Calculation of dead carbon proportion. Radiocarbon 39, 33–48.

Genty, D., Massault, M., Gilmour, M., Baker, A., Verheyden, S., Kepens, E., 1999. Calculation of past dead carbon proportion and variability by the comparison of AMS ^{14}C and TIMS U/Th ages on two Holocene stalagmites. Radiocarbon 41, 251–270.

Goede, A., 1994. Continuous early last glacial palaeoenvironmental record from a Tasmanian speleothem based on stable isotope and minor elements variations. Quaternary Science Reviews 13, 283–291.

Hellstrom, J., McCulloch, M., 2000. Multi-proxy constraints on the climatic significance of trace element records from a New Zealand speleothem. Earth and Planetary Science Letters 179, 287–297.

Hellstrom, J., McCulloch, M., Stone, J., 1998. A detailed 31,000 year record of climate and vegetation change, from the isotope geochemistry of two New Zealand speleothems. Quaternary Science 50, 167–178.

Hendy, C.H., 1971. The isotopic geochemistry of speleothems-I. The calculation of the effects of different modes of formation on the isotopic composition of speleothems and their applicability as palaeoclimatic indicators. Geochimica et Cosmochimica Acta 35, 801–824.

Hillaire-Marcel, C., Causse, C., 1989. Chronologie Th/U des concretions calcaires des varves du lac glaciaire de Deschaillons (Wisconsinien inferieur). Canadian Journal of Earth Sciences 26, 1041–1052.

Hillaire-Marcel, C., Ghaleb, B., Gariepy, C., Zazo, C., Hoyos, M., Goy, J.L., 1995. U-series dating by the TIMS technique of land snails from paleosols in the canary islands. Quaternary Research 44, 276–282.

Hillaire-Marcel, C., Ghaleb, B., Simonetti, A., Gariepy, C., 2000. Western boundary undercurrent control of Th-isotope fluxes in the Labrador Sea based on MC-ICP-MS measurements of total ^{230}Th and ^{232}Th in 5 litre water samples. Goldschmidt Conference, September 3–8th 2000, Oxford, UK.

Johnsen, S.J., Clausen, H.B., Dansgaard, W., Fuhrer, K., Gundestrup, N., Hammer, C.U., Iversen, P., Jouzel, J., Stauffer, B., Steffensen, J.P., 1992. Irregular glacial interstadials recorded in a new Greenland ice core. Nature 359, 311–313.

Kaufman, A., 1993. An evaluation of several methods for determining $^{230}Th/U$ ages in impure carbonates. Geochimica et Cosmochimica Acta 57, 2303–2317.

Kaufman, A., Broecker, W.S., 1965. Comparison of ^{230}Th and ^{14}C ages for carbonate material from Lahontan and Bonneville. Journal of Geophysical Research 70, 4039–4054.

Kaufman, A., Wasserburg, G.J., Porcelli, D., Bar-Matthews, M., Ayalon, A., Halicz, L., 1998. U-Th isotope systematics from the Soreq Cave, Israel, and climatic correlations. Earth and Planetary Science Letters 156, 141–155.

Ku, T.L., Bull, W.B., Freeman, S.T., Knauss, K.G., 1979. $^{230Th}\_^{234}U$ dating of pedogenic carbonates in gravelly desert soils of Vidal Valley, Southern California. Geological Society of America Bulletin 90, 1063–1073.

Latham, A.G., Schwarcz, H.P., Ford, D.C., 1986. The paleomagnetism and U–Th dating of Mexican stalagmite, DAS2. Earth and Planetary Science Letters 79, 195–207.

Lauritzen, S.E., 1995. High resolution paleotemperature proxy record for the last interglaciation based on Norwegian speleothems. Quaternary Research 43, 133–146.

Li, W.X., Lundberg, J., Dickin, A.P., Ford, D.C., Schwarcz, H.P., McNutt, R., Williams, D., 1989. High-precision mass spectrometric uranium series dating of cave deposits and implications for palaeoclimates studies. Nature 339, 534–536.

Ludwig, K.R., Simmons, K.R., Szabo, B.J., Winograd, I.J., Landwher, J.M., Riggs, A.C., Hoffman, R.J., 1992. Mass-spectrometric $^{230}Th–^{234}U–^{238}U$ dating of the Devils Hole calcite vein. Science 258, 284–287.

Luo, S., Ku, T.L., 1991. U-series isochron dating: A generalized method employing total-sample dissolution. Geochimica et Cosmochimica Acta 55, 555–564.

Moure-Romanillo, J.A., Cano-Herrera, M., 1979. Tito bustillo cave (Asturias, Spain) and the Magdalenian of Cantabria. World Archaeology 10, 280–289.

Penalba, M.C., Arnold, M., Guiot, J., Duplessy, J.C., de Beaulieu, J.L., 1997. Termination of the last glaciation in the Iberian Peninsula inferred from the pollen sequence of Quintanar de la Sierra. Quaternary Research 48, 205–214.

Rihs, S., Poidevin, J.L., Condomines, M., 1999. Premiers ages U-Th sur la grotte des Demoiselles (Hérault): Evolution karstique et relation paléclimatique. Quaternaire 10, 293–297.

Rosholt, J.N., 1976. $^{230}Th/^{234}U$ dating of travertine and caliche rinds. GSA Abstract Program 8, 1076.

Schwarcz, H.P., Latham, A.G., 1989. Dirty calcite. 1-Uranium-series dating of contaminated calcite using leachates alone. Chemical Geology 80, 35–43.

Shackleton, N.J., 1987. Oxygen isotopes, ice volume and sea-level. Quaternary Science Reviews 6, 183–190.

Stein, M., Wasserburg, G.J., Aharon, P., Chen, J.H., Zhu, Z.R., Bloom, A., Chappell, J., 1993. TIMS U-series dating and stable isotopes of the last interglacial event in Papua New Guinea. Geochimica et Cosmochimica Acta 57, 2541–2554.

Straus, L.G., 1975–76. The upper paleolithic cave site of Altamira (Santander, Spain). Quaternaria 19, 135–147.

Stuiver, M., Reimer, P.J., Bard, E., Beck, J.W., Burr, G.S., Hughen, K.A., Kromer, B., McCormac, G., Van der Plicht, J., Spurk, M., 1998. INTCAL98 radiocarbon age calibration, 24,000 cal BP. Radiocarbon 40, 1041–1083.

Valladas, H., Cachier, H., Maurice, P., Bernaldo de Quiros, F., Clottes, J., Cabrera Valdes, V., Uzquiano, P., Arnold, M., 1992. Direct radiocarbon dates for prehistoric paintings at the Altamira, El Castillo, and Niaux Caves. Nature 357, 68–70.

Vesica, P.L., Tuccimei, P., Turi, B., Fornos, J.J., Gines, A., Gines, A., 2000. Late Pleistocene paleoclimates and sea-level change in the Mediterranean as inferred from stable isotope and U-series studies of overgrowths on speleothems, Mallorca, Spain. Quaternary Science Reviews 19, 865–879.

Wansard, G., 1996. Quantification of paleotemperature changes during isotopic stage 2 in the La Draga continental sequence based on the Mg/Ca ratio of freshwater ostracods. Quaternary Science Reviews 15, 237–245.

Winograd, I.J., Coplen, T.B., Landwehr, J.M., Riggs, J.M., Ludwig, K.R., Szabo, B., Kolesar, P.T., Revesz, K.M., 1992. Continuous 500,000 years climate record from vein calcite in Devils Hole, Nevada. Science 258, 255–260.